JACC: CARDIOVASCULAR IMAGING VOL. 3, NO. 2, 2010

ISSN 1936-878X/10/$36.00
PUBLISHED BY ELSEVIER INC. DOI:10.1016/j.jcmg.2009.11.004

OCT Assessment of Thin-Cap Fibroatheroma Distribution in Native Coronary Arteries

Kenichi Fujii, MD,* Daizo Kawasaki, MD,* Motomaru Masutani, MD,† Takahiro Okumura, MD,† Takafumi Akagami, MD,† Tsuyoshi Sakoda, MD,† Takeshi Tsujino, MD,* Mitsumasa Ohyanagi, MD,† Tohru Masuyama, MD*

Nishinomiya, Japan

OBJECTIVES We evaluated the geographic distribution of thin-cap fibroatheromas (TCFAs) in the coronary arteries using optical coherence tomography (OCT), a high-resolution imaging modality.

BACKGROUND Plaque rupture is the most frequent cause of acute myocardial infarction (AMI). It has been recognized that TCFA is the primary plaque type at the site of plaque rupture.

METHODS We performed 3-vessel OCT examinations in 55 patients: 35 AMI and 20 stable angina pectoris patients. The criteria for TCFA in an OCT image was a lipid-rich plaque with fibrotic cap thickness <65 μm. The distance between each TCFA location and the respective coronary artery ostium was measured with motorized OCT imaging pullback. The total length of all 3 coronary arteries imaged by OCT pullbacks was 82 $\pm$ 21 mm in the left anterior descending coronary artery (LAD), 67 $\pm$ 26 mm in the left circumflex coronary artery (LCx), and 104 $\pm$ 32 mm in the right coronary artery (RCA).

RESULTS OCT detected 94 TCFAs in 165 coronary arteries. The minimum fibrous-cap thickness of TCFAs was 57.4 $\pm$ 5.4 μm in AMI patients, and 55.9 $\pm$ 7.3 μm in stable angina pectoris patients ($p = 0.4$). Of the total of 94 TCFAs, 28 were detected in the LAD, 18 in the LCx, and 48 in the RCA. Most LAD TCFAs were located between 0 and 30 mm from the LAD ostium (76%). Conversely, LCx and RCA TCFAs were evenly distributed throughout the entire coronary length. The clustering of the TCFAs was similar in culprit segments as compared with nonculprit segments. In AMI patients, most LAD TCFAs were distributed near side branches, mainly positioned opposite the side branch bifurcation.

CONCLUSIONS Three-vessel OCT imaging showed that TCFAs tend to cluster in predictable spots within the proximal segment of the LAD, but develop relatively evenly in the LCx and RCA arteries. (J Am Coll Cardiol Img 2010;3:168–75) © 2010 by the American College of Cardiology Foundation

From the *Cardiovascular Division and the †Division of Coronary Heart Disease, Hyogo College of Medicine, Nishinomiya, Japan.

Manuscript received July 6, 2009; revised manuscript received October 19, 2009, accepted November 6, 2009.

Plaque rupture with subsequent thrombus formation is the most frequent cause of acute coronary syndromes, such as acute myocardial infarction (AMI) (1–3). Recently, it has been reported that several vulnerable plaques other than the "culprit" stenosis can be found in individual patients with AMI (4,5) and that multiple plaque ruptures occur in patients with acute coronary syndrome (6,7). These findings are likely to be the result of a diffuse inflammatory process that leads to multifocal plaque instability. Therefore, it is now widely recognized that inflammation influences the presence of vulnerable plaques, and thus plaque instability may reflect a pancoronary process. However, a previous angiographic study demonstrated that coronary thromboses tend to develop at "hot spots" within the proximal third of each coronary artery (8).

It has been postulated that thin-cap fibroatheromas (TCFAs), which are characterized by a large lipid core with an overlying thin fibrous cap measuring <65 μm, are the precursor plaque composition of later plaque ruptures (9–11). However, current imaging modalities such as angiography, intravascular ultrasound (IVUS), and angioscopy cannot screen for or assess TCFAs accurately due to their insufficient resolution. Optical coherence tomography (OCT) imaging has recently been introduced for in vivo human imaging and offers a higher resolution than any other available imaging modality, allowing for the reliable and reproducible assessment of TCFAs (12,13).

The current study utilized OCT to evaluate whether TCFAs, the precursors to intracoronary plaque rupture and subsequent thrombosis, are focally or diffusely distributed in all 3 native coronary arteries in patients with AMI and stable angina pectoris (SAP).

METHODS

Study population. A prospective but nonconsecutive series of 60 patients who were scheduled for percutaneous coronary intervention (PCI) underwent OCT examination of all 3 epicardial coronary arteries. Forty had AMI and 20 had SAP. Patients with 3-vessel disease, a history of myocardial infarction, and severe left ventricular dysfunction were not enrolled because of the potential difficulty in acquiring and interpreting OCT images with such conditions. AMI was defined as continuous chest pain at rest with abnormal levels of creatine kinase-MB. All AMI patients had ST-segment elevation (>0.1 mV in 2 contiguous electrocardiogram [ECG] leads), and primary PCI was attempted within 6 h of symptom onset. The mean duration from AMI onset to OCT examination was 4.6 ± 1.0 h. SAP was defined as no change in frequency or intensity of symptoms within 6 weeks. Identification of culprit/target lesions involved the combination of left ventricular wall motion abnormalities, ECG findings, angiographic lesion morphology, and scintigraphic defects (6,12). All patients provided written informed consent, and approval of the presiding ethical committee was obtained.

OCT imaging protocol and analysis. A 0.016-inch wire-type imaging catheter (ImagingWire, LightLab Imaging, Westford, Massachusetts) was advanced to the culprit/target lesion through a 4-F over-the-wire occlusion balloon catheter (Helios, Goodman Co, Nagoya, Japan). Then, the occlusion balloon was inflated to 0.4 to 0.6 atm while lactated Ringer's solution was infused from the balloon tip at 0.5 ml/s to flush blood from the imaging field. An imaging run was performed from the distal segment to the proximal segment of the culprit/target lesion using automated pullback at 1.0 mm/s. After the treatment of the culprit/target lesion, OCT examinations of the nonculprit/nontarget lesions of all 3 coronary arteries were performed. The arteries were imaged continuously over a 20- to 50-mm length from the distal segment to the ostium. Only the most proximal 3-mm segments of the arteries, which were obscured by the occlusion balloon, were not imaged by OCT.

ABBREVIATIONS AND ACRONYMS

AMI = acute myocardial infarction
IVUS = intravascular ultrasound
LAD = left anterior descending coronary artery
LCx = left circumflex coronary artery
OCT = optical coherence tomography
RCA = right coronary artery
SAP = stable angina pectoris
TCFA = thin-cap fibroatheroma

OCT images were analyzed by 2 independent observers who were blinded to the clinical presentations. Said analysis was performed using proprietary software from LightLab Imaging and validated criteria for plaque characterization (6,14). For all plaques with an OCT-determined lipid core, the fibrous cap thickness was measured at its thinnest part. If the fibrous cap of a given plaque was visible, cap thicknesses were measured 5 times, and the average of the 3 middle values was calculated. The size of a lipid lesion was quantified according to the arc of the lipid tissue as it appeared in quadrants of the cross-sectional OCT image. When lipid was present in ≥1 quadrant in any of the images within a plaque, it was considered a lipid-rich plaque. A TCFA was defined by OCT analysis as a plaque with lipid content in ≤1 quadrant and the thinnest part of a fibrous cap measuring ≤65 μm (6). A

representative case is shown in Figure 1. For TCFAs located in the left anterior descending coronary artery (LAD), transversal distribution of the associated lipid core was evaluated. The cross-section displaying the largest lipid core within each detected TCFA was divided into myocardial and pericardial surfaces using the take-off of a septal branch emerging on the side of the vessel opposite the pericardium (15,16). The transverse distribution of TCFAs was considered pericardial if the lipid core area on the pericardial surface was larger than that on the myocardial surface. A plaque rupture was defined as a plaque containing a cavity that communicated with the lumen with an overlying residual fibrous cap fragment.

Statistical analyses. Data are presented as frequencies or mean ± 1 SD. Comparison was performed with unpaired Student *t* test and chi-square test. Interobserver variability was quantified using kappa concordance analysis for plaque characterization. A p value of <0.05 was considered statistically significant. There were no corrections made in these analyses for correlated observations in the same patient.

RESULTS

Baseline patient characteristics and frequency of TCFA. Of 60 patients, 3 AMI patients were excluded from analysis because Thrombolysis In Myocardial Infarction flow grade 3 was not achieved. Two AMI patients were also excluded from analysis because 1 or 2 coronary arteries were not successfully imaged by OCT. Accordingly, a total of 55 patients (35 AMI and 20 SAP patients) were prospectively included in the study. Baseline clinical characteristics are shown in Table 1.

There were 32 culprit/target TCFAs and 62 nonculprit/nontarget TCFAs. The mean value for the minimum fibrous-cap thickness within TCFAs was 57.4 ± 5.4 μm in AMI patients, and 55.9 ± 7.3 μm in SAP patients (p = 0.4). A total of 94 TCFAs were detected in 165 coronary arteries: 28 TCFAs in the LAD, 18 in the left circumflex coronary arteries (LCx), and 48 in the right coronary arteries (RCA). The total length of all 3 coronary arteries imaged by OCT pullbacks was 82 ± 21 mm in the LAD, 67 ± 26 mm in the LCx, and 104 ± 32 mm in the RCA. Interobserver variability yielded acceptable concordance for TCFA (kappa = 0.88). Angiographic appearance of nonculprit TCFAs with AMI patients was normal in 12 lesions (22%), hazy in 5 (9%), and critical stenosis (>50% of diameter stenosis) in 22 (41%). Similarly, angiographic appearance of nontarget TCFAs with SAP patients was normal in 5 lesions (63%), hazy in 1 (13%), and critical stenosis (>50% of diameter stenosis) in 1 (13%).

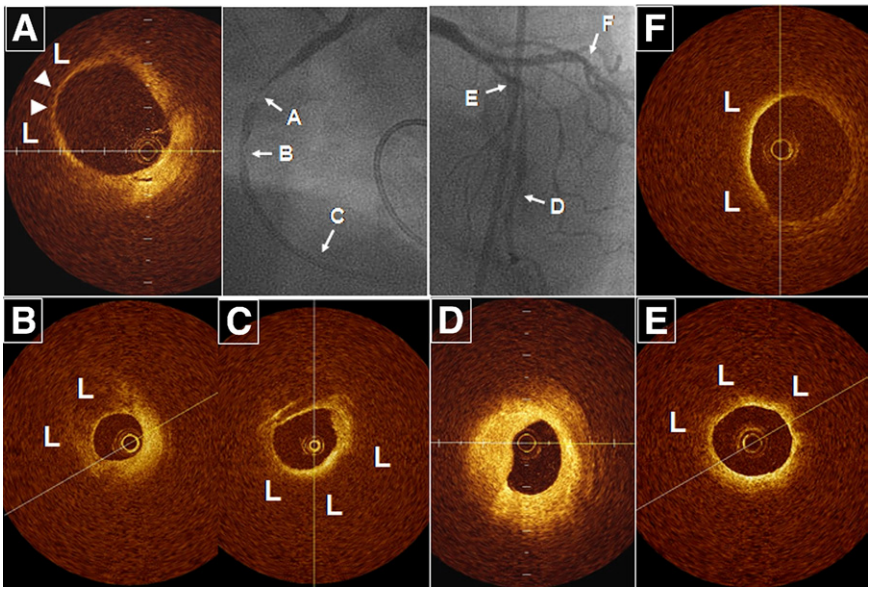

Figure 1. OCT in Culprit and Nonculprit Lesions

(A) Optical coherence tomography (OCT) image of the culprit lesion with lipid-rich (L) plaque covered by a thin-fibrous cap (53.3 μm) **(arrowheads)** indicates thin-cap fibroatheroma (TCFA). **(B, C, E, and F)** TCFAs were also observed in the nonculprit segments. **(D)** OCT image of a fibrous plaque showing a homogeneous and signal-rich interior was observed.

Table 1. Baseline Clinical Characteristics (n = 35)

Age, yrs	67 ± 11
Male	34 (62)
Hypertension	36 (65)
Hypercholesterolemia	36 (65)
Diabetes mellitus	21 (38)
Cigarette smoking	12 (22)
Lipid profiles, mg/dl	
Total cholesterol	205 ± 38
LDL cholesterol	122 ± 31
HDL cholesterol	52 ± 12
Triglycerides	127 ± 70
Family history of CAD	15 (27)
Target coronary artery, %	
Left anterior descending	26 (47)
Left circumflex	8 (15)
Right	21 (38)
Angiographic analysis, mm	
Reference segment	3.2 ± 0.8
Minimum lumen diameter	0.4 ± 0.6
Multivessel disease	16 (29)

Values are given as n (%) or mean ± SD.
CAD = coronary artery disease; HDL = high-density lipoprotein; LDL = low-density lipoprotein.

Spatial distribution of TCFAs. The distance between minimum fibrous-cap thickness site and coronary ostium was 22 ± 12 mm in the LAD, 32 ± 18 mm in the LCx, and 41 ± 26 mm in the RCA. Frequency distribution is shown in Figure 2. LAD TCFAs were predominantly located in the proximal segment: the first 30 mm from the LAD ostium (76%, 22 of 29) and the first 40 mm from the LAD ostium (97%, 28 of 29). LCx TCFAs were evenly distributed throughout the length of the LCx that was imaged: only 47% (8 of 17) of LCx TCFAs were located within the first 30 mm from the ostium. RCA TCFAs were also evenly distributed throughout the length of the RCA that was imaged: only 42% (20 of 48) of RCA TCFAs were located within the first 30 mm from the ostium. The distribution pattern was similar in culprit/target TCFAs compared to nonculprit/nontarget TCFAs (Fig. 3).

In 51% (48/94) of TCFAs, there was a side branch (>1.0 mm of reference diameter on angiogram) near the minimum fibrous-cap thickness site of TCFAs (29 proximal and 19 distal to the side branch); 76% (22 of 29) in the LAD, 47% (8 of 17) in the LCx, and 38% (18 of 48) in the RCA. The mean distance between minimum fibrous-cap thickness site and the side branch measured 2.0 ± 1.4 mm.

Spatial distribution of ruptured plaques. Infarct-related lesion plaque rupture was found in 16 (46%) AMI patients, and target lesion plaque rupture was found in 2 (10%) SAP patients (p = 0.008). There was ≥1 noninfarct-related/nontarget plaque rupture in 11 (31%) AMI patients and 3 (15%) SAP patients (p = 0.2). The distance between minimum fibrous-cap thickness site and coronary ostium was 16 ± 8 mm in the LAD, 49 ± 27 mm in the LCx, and 43 ± 23 mm in the RCA. Frequency distribution is shown in Figure 4. Most LAD ruptured plaques were clustered in the proximal segment, and

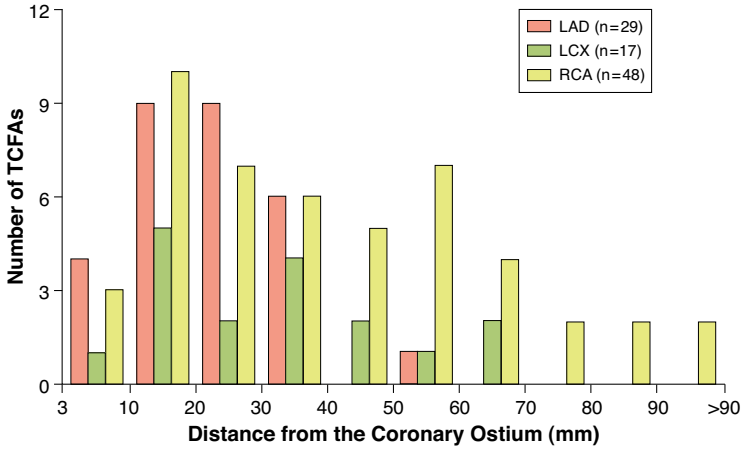

Figure 2. Frequency of TCFAs According to Distance From Coronary Ostium

The frequency of 94 thin-cap fibroatheromas (TCFAs) according to distance from each coronary ostium is shown for the left anterior descending artery (LAD), the left circumflex artery (LCx), and the right coronary artery (RCA). Most LAD and LCx TCFAs tend to cluster in the proximal segments of the artery.

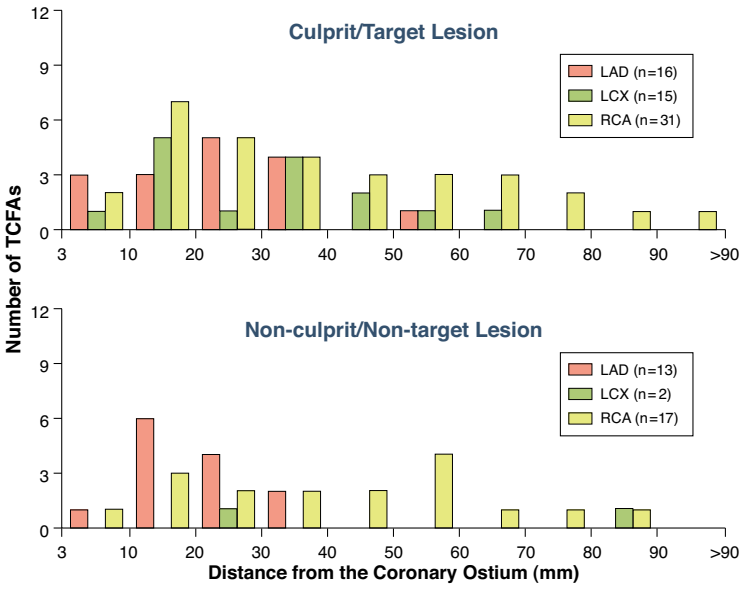

Figure 3. Frequency Distribution of TCFA at Culprit and Nonculprit Lesions

The frequency distribution of thin-cap fibroatheromas (TCFAs) according to distance from each coronary ostium is shown for the left anterior descending coronary artery (LAD), the left circumflex coronary artery (LCx), and the right coronary artery (RCA). Culprit and nonculprit lesions are shown separately. The distribution pattern was similar in culprit TCFAs as compared with nonculprit TCFAs.

RCA plaque ruptures were evenly distributed throughout the entire coronary length.

Spatial and transversal distribution of LAD TCFAs in AMI patients. In the LAD, 27 plaques that did not display the OCT criteria for TCFA were also identified during the OCT examinations. The distribution pattern in the LAD was significantly different between 26 TCFAs and 27 non-TCFAs (Fig. 5). The average distance from each plaque to LAD ostium was significantly shorter in TCFAs compared to non-TCFAs (22 ± 13 vs. 39 ± 15 mm, $p < 0.001$).

In AMI patients, 20 of 26 LAD TCFAs (77%) were located near the side branch (14 proximal and

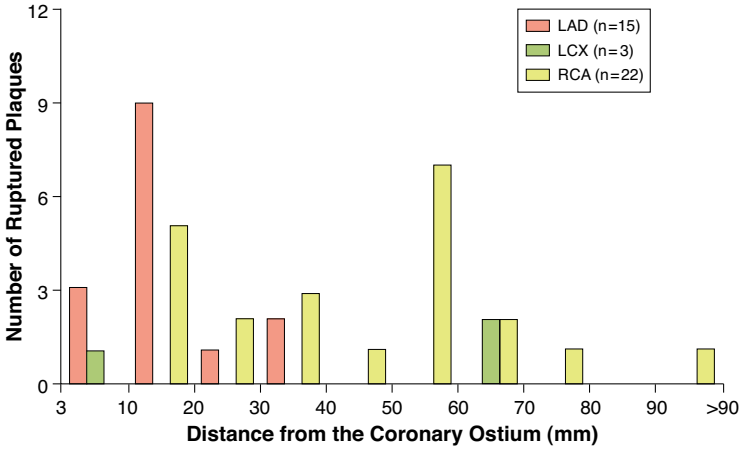

Figure 4. Frequency of Ruptured Plaques According to Distance From Each Coronary Ostium

The frequency of ruptured plaques according to distance from each coronary ostium is shown. The distribution pattern of ruptured plaques was similar to that of thin-cap fibroatheromas. Most left anterior descending coronary artery (LAD) ruptured plaques were located in the proximal segments of the artery. Right coronary artery (RCA) ruptured plaques were evenly distributed throughout the entire coronary length. LCx = left circumflex coronary artery.

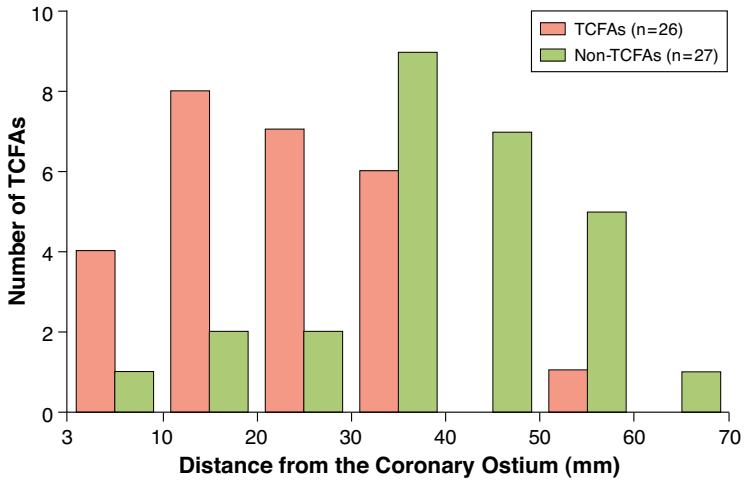

Figure 5. Frequency Distribution of TCFAs and Non-TCFAs Located in the LAD According to Distance From Coronary Ostium

The frequency distribution of thin-cap fibroatheromas (TCFAs) and non-TCFAs located in the left anterior descending coronary artery (LAD) according to distance from each coronary ostium. The distribution pattern in the left anterior descending artery was significantly different between 26 TCFAs and 27 non-TCFAs. The average distance from each plaque to LAD ostium was significantly shorter in TCFAs compared to non-TCFAs.

6 distal to the side branch). The distance between minimum fibrous-cap thickness site and the side branch measured on average 1.5 ± 1.1 mm.

In the 54% of LAD TCFAs observed near the diagonal branch, the lipid core was located opposite the diagonal branch in 57%, adjacent in 43%, and concordant in 0%. Of the 14 TCFAs located near the diagonal branch, 13 (93%) had a pericardial and only 1 (7%) a myocardial distribution. Similarly, in the 23% of LAD TCFAs observed near the septal branch, the lipid core was located opposite the septal branch take-off in 50%, perpendicular in 17%, and concordant in 33%. Of the 6 TCFAs located near the septal branch, 4 (75%) had a pericardial and 2 (25%) had a myocardial distribution.

DISCUSSION

With 3-vessel OCT imaging, we evaluated the distribution of TCFAs in the native coronary arteries of 55 patients with both AMI and SAP. TCFAs were clustered in the proximal segments of the LAD, but distributed relatively evenly through the entire LCx and RCA arterial lengths. In AMI patients, most TCFAs located in the LAD were oriented toward the pericardial side or opposite the side branch bifurcation.

Our results are in accordance with previous pathological observations (17), which showed that TCFAs were found in the proximal LAD, proximal and middle RCA, and proximal and middle LCx. This pathological evidence fits well with the angiographic study demonstrating that epicardial coronary thrombosis tends to cluster within the proximal third of each coronary artery (8). This current OCT study agrees with Wang et al. (8) regarding the proximal distribution of the LAD and midsegment distribution of the RCA.

However, in this study, LCx TCFAs were distributed evenly through the length of the LCx that was imaged by OCT. Possible reasons for the discrepancy between the current OCT study and the previous angiographic and autopsy studies are not entirely clear; one explanation may include differences between study populations. In this study, patients with triple-vessel disease were excluded because of the potential difficulty in acquiring OCT images. This selection bias might affect the discrepancy. The angiographic study enrolled only patients with acute vessel occlusion, regardless of the underlying plaque pathology, and furthermore enrolled only culprit lesions, whereas our current OCT study included all TCFAs regardless of clinical consequences. It is well known that coronary events, such as plaque rupture and erosion, can occur not only at culprit lesions, but also at nonculprit lesions.

In line with the current study, previous IVUS studies revealed that LAD plaque ruptures predominantly occurred in the proximal segments, whereas LCx plaque ruptures were evenly distributed in the LCx tree (18). Detection of plaques with complex

morphology, such as previously ruptured plaques, may be more precise with OCT than with IVUS because the higher resolution of OCT permits better differentiation of heterogeneous plaque composition. The 10-μm resolution of OCT allows the reviewer not only to identify plaques that have already ruptured and subsequently healed, but also to identify plaques that may be prone to rupture due to a TCFA structure (12,13).

There are several possible explanations for the spatial distribution of TCFAs. The distribution of TCFAs seems to resemble the distribution of coronary atherosclerosis as assessed with IVUS (19), as well as the larger arterial diameter present in the proximal LAD and LCx and throughout the RCA. The segments identified in this study might be points of vessel tortuosity and frequent branching, resulting in significant variations in shear stress as compared with other arterial segments (20). Shear stress affects endothelial damage and cap fatigue, both of which may contribute to plaque vulnerability (21). Furthermore, disturbed shear stress influences the site selectivity of atherosclerotic plaque formation as well as its associated vessel wall remodeling, which can contribute to plaque vulnerability, such as the development of TCFAs (20).

In the current study, 51% of TCFAs were located near a side branch, particularly in the LAD (76%), which may cause flow instability. The side branch affects shear stress distribution in the associated main branch by diminishing it in the region within 3 mm of the side branch (22). Such regions in the main branch were identified both proximal and distal to the side branch (24). In addition, a previous study reported that endothelial cells near side branches have a reduced ability to repair wounds compared with endothelial cells residing in nonbranch regions (23). In this study, the lipid core within identified TCFAs was mainly located opposite the side branch bifurcation in the LAD. In these geometrically predisposed locations, shear stress on the vessel wall is significantly lower in magnitude and exhibits directional changes and flow separation (24). Low shear stress enhances the oxidation of lipids and their accumulation (25), possibly contributing to the formation of lipid pools during the development of atherosclerosis plaques.

The interplay among systemic and local factors contributing to the progression and vulnerability of atherosclerotic coronary lesions should be concentrated on in an attempt to control the chronic and acute consequences of coronary atherosclerosis (26). Thus the finding that coronary plaques show a vulnerable morphology if proximally located along the longitudinal axis of the vessel in comparison to those more distally located in the same artery, especially in the LAD of AMI patients, might allow development of more aggressive strategies for prevention of secondary coronary events in AMI.

Study limitations. Further studies are required to reconfirm the results in a larger number of patients. Because the proximal segments of the target coronary arteries had to be occluded to remove blood from the imaging field, real ostial segments were not imaged. Although OCT imaging was performed in all 3 coronary arteries, some distal segments of each coronary artery were not imaged due to tortuosity. Because the transversal distribution of TCFAs was only analyzed in the LAD, we cannot speculate whether TCFAs were mainly distributed relative to the side branch bifurcation or pericardium side in the same manner in the other 2 coronary arteries. The transversal distribution of plaques could not be analyzed accurately in the LCx and RCA because these arteries had fewer side branches compared with the LAD. Some TCFAs at the infarct-related lesion of AMI patients might be missed due to large intramural thrombus covering the plaque. Finally, coronary thrombectomy before the OCT examination might affect the morphologic features of the infarct-related lesion.

CONCLUSIONS

Three-vessel OCT imaging showed that pre-rupture TCFAs tend to cluster in predictable hot spots within the proximal segments of the LAD but are evenly distributed throughout the entire LCx and RCA.

Acknowledgments

The authors thank the staff in the coronary care unit and the cardiac catheterization laboratory at Hyogo College of Medicine for their excellent assistance during the study.

Reprint requests and correspondence: Dr. Kenichi Fujii, Hyogo College of Medicine, Cardiovascular Division, 1-1 Mukogawa-cho, Nishinomiya-city, Hyogo 6638501, Japan. *E-mail: kfujii@hyo-med.ac.jp.*

REFERENCES

1. Davies M, Thomas A. Thrombosis and acute coronary artery lesions in sudden cardiac ischemic death. N Engl J Med 1984;310:1137–40.
2. Fuster V, Badimon L, Badimon JJ, Chesebro JH. The pathogenesis of coronary artery disease and the acute coronary syndromes. N Engl J Med 1992;326:242–50,310–8.
3. Virmani R, Kolodgie FD, Burke AP, Farb A, Schwartz SM. Lessons from sudden coronary death: a comprehensive morphological classification scheme for atherosclerotic lesions. Arterioscler Thromb Vasc Biol 2000;20:1262–75.
4. Asakura M, Ueda Y, Yamaguchi O, et al. Extensive development of vulnerable plaques as a pan-coronary process in patients with myocardial infarction: an angioscopic study. J Am Coll Cardiol 2001;37:1284–8.
5. Goldstein JA, Demetriou D, Grines CL, Pica M, Shoukfeh M, O'Neill WW. Multiple complex coronary plaques in patients with acute myocardial infarction. N Engl J Med 2000; 343:915–22.
6. Hong MK, Mintz GS, Lee CW, et al. Comparison of coronary plaque rupture between stable angina and acute myocardial infarction: a three-vessel intravascular ultrasound study in 235 patients. Circulation 2004;110:928–33.
7. Rioufol G, Finet G, Ginon I, et al. Multiple atherosclerotic plaque rupture in acute coronary syndrome: a three-vessel intravascular ultrasound study. Circulation 2002;106:804–8.
8. Wang JC, Normand SL, Mauri L, Kuntz RE. Coronary artery spatial distribution of acute myocardial infarction occlusions. Circulation 2004; 110:278–84.
9. Virmani R, Kolodgie FD, Burke AP, Farb A, Schwartz SM. Lessons from sudden coronary death: a comprehensive morphological classification scheme for atherosclerotic lesions. Arterioscler Thromb Vasc Biol 2000;20:1262–75.
10. Fuster V, Stein B, Ambrose JA, Badimon L, Badimon JJ, Chesebro JH. Atherosclerotic plaque rupture and thrombosis. Evolving concepts. Circulation 1990;82 Suppl:II47–59.
11. Naghavi M. From vulnerable plaque to vulnerable patient: a call for new definitions and risk assessment strategies: part 1. Circulation 2003;108: 1664–72.
12. Jang IK, Tearney GJ, MacNeill B, et al. In vivo characterization of coronary atherosclerotic plaque by use of optical coherence tomography. Circulation 2005;111:1551–5.
13. Kume T, Akasaka T, Kawamoto T, et al. Measurement of the thickness of the fibrous cap by optical coherence tomography. Am Heart J 2006;152: 755.e1–4.
14. Yabushita H, Bouma BE, Houser SL, et al. Characterization of human atherosclerosis by optical coherence tomography. Circulation 2002;106:1640–5.
15. Fitzgerald PJ, Yock C, Yock PG. Orientation of intracoronary ultrasonography: looking beyond the artery. J Am Soc Echocardiogr 1998;11: 13–9.
16. Prati F, Arbustini E, Labellarte A, et al. Eccentric atherosclerotic plaques with positive remodelling have a pericardial distribution: a permissive role of epicardial fat? A three-dimensional intravascular ultrasound study of left anterior descending artery lesions. Eur Heart J 2003;24:329–36.
17. Kolodgie FD, Burke AP, Farb A, et al. The thin-cap fibroatheroma: a type of vulnerable plaque: the major precursor lesion to acute coronary syndromes. Curr Opin Cardiol 2001;16; 285–92.
18. Hong MK, Mintz GS, Lee CW, et al. The site of plaque rupture in native coronary arteries: a three-vessel intravascular ultrasound analysis. J Am Coll Cardiol 2005;46:261–5.
19. Tinana A, Mintz GS, Weissman NJ. Volumetric intravascular ultrasound quantification of the amount of atherosclerosis and calcium in nonstenotic arterial segments. Am J Cardiol 2002;89:757–60.
20. Cunningham KS, Gotlieb AI. The role of shear stress in the pathogenesis of atherosclerosis. Lab Invest 2005;85: 9–23.
21. Feldman CL, Stone PH. Intravascular hemodynamic factors responsible for progression of coronary atherosclerosis and development of vulnerable plaque. Curr Opin Cardiol 2000;15:430–40.
22. Gijsen FJ, Wentzel JJ, Thury A, et al. A new imaging technique to study 3-D plaque and shear stress distribution in human coronary artery bifurcations in vivo. J Biomech 2007;40: 2349–57.
23. Akong TA, Gotlieb AI. Reduced in vitro repair in endothelial cells harvested from the intercostal ostia of porcine thoracic aorta. Arterioscler Thromb Vasc Biol 1999;19:665–71.
24. Zarins CK, Giddens DP, Bharadvaj BK, Sottiurai VS, Mabon RF, Glagov S. Carotid bifurcation atherosclerosis: quantitative correlation of plaque localization with flow velocity profiles and wall shear stress. Circ Res 1983; 53:502–14.
25. Malek AM, Alper SL, Izumo S. Hemodynamic shear stress and its role in atherosclerosis. JAMA 1999;282:2035–42.
26. VanderLaan PA, Reardon CA, Getz GS. Site specificity of atherosclerosis: site-selective responses to atherosclerotic modulators. Arterioscler Thromb Vasc Biol 2004;24:12–22.

Key Words: optical coherence tomography ■ vulnerable plaque ■ acute coronary syndrome.